

International Conference on
COMPUTER INTEGRATED MANUFACTURING
Internationale Konferenz über
RECHNERINTEGRIERTE FERTIGUNGSSYSTEME
Zakopane, March 24-27 1992

Jożef KNAPCZYK^{*} and Andrzej STEPNIIEWSKI^{**}

^{*}Cracow University of Technology, Cracow, Poland

^{**}Lublin Academy of Agriculture, Lublin, Poland

SOME EFFECTS OF THE JOINT'S DRIVE SYSTEMS TORSIONAL COMPLIANCES
AND THE VELOCITY PROFILES ON THE 5R MANIPULATOR'S DYNAMIC ACCURACY

Summary. The dynamic model of the 5R manipulator has been developed and applied for the IRb-60 manipulator. The Lagrange's 2nd order equations for each link are derived including torsional compliances for the 4th and 5th joint driven by the steel band transmission systems. The coefficients of the joint drive systems compliances have been calculated on the basis of the static measurement results. The end-effector oscillations measured by using piezoelectric accelerometer are compared with the results of computer simulation. The effects of the joint compliances and velocity profiles have been analysed.

1. Introduction

Usually the fundamental natural (resonance) frequencies of joint drive systems are relatively low ($2 + 30$ Hz), the natural periods ($0,5 + 0,03$ s) are close to the duration of the transient motions associated with regional or local motions (e.g. deceleration of the manipulator arm). Low stiffness (high compliance) values lead to longer stabilization time and reduce performance characteristics especially if inertia forces are high, thus reduce accuracy and repeatability. For continuous path operations or forcecontrolled inspection operations, enhanced compliance is desirable. The best design is one which allows for controlled stiffness and compliance.

Compliant connections effectively increase the number of DOF in addition to degree of freedom for "gross" (programmable) motions, there are degrees of freedom associated with link oscillations relative to their programmed positions. Since equations of manipulator motion are quite complex, the full equations including compliance are much more cumbersome. They are also highly nonlinear and contain many coupling terms. However, as it is shown in [4], the compliances of joints, actuators, and transmission systems, which can be reduced to joints, usually represent 70% or more of total compliance of manipulator.

Compliance is an inherent characteristics of position-controlled robots. The amount of available compliance depends on robot design. Structural compliance can arise due to the stiffness of the manipulator links as well as joint drive systems. The robot arm members are normally quite massive and can be regarded as rigid links. The bearings and wrist parts are also assumed to be rigid because the joint drive systems have quite large torsional deflections in comparison [1].

The end-effector compliance characteristics can be derived as a function of manipulator kinematic and dynamic parameters, and torsional compliance of individual joint. The emerging trend for compliant and light robot with higher payload capacities, and the use of relatively flexible components of the joint drive systems such as steel band transmission strongly suggested that these compliances need to be considered for a realistic system representation. To apply the compliance model to the robot manipulator the coefficients of joint drive system compliances are needed. Theoretically these could be obtained on the basis of the actual drive system specifications. However, since the data for joint drive systems were not available from the robot manufacturer it is necessary to measure the compliances directly [2].

This paper presents the 6R manipulator's dynamic model useful for prediction the end-effector trajectory errors caused by the compliances of the joint drive systems. As an example the dynamic model of the IRb-60 manipulator with the 4th and 5th joints driven by the steel band transmission systems is analyzed. The measured compliances are used in this model to describe the dynamic accuracy of the end-effector trajectory.

2. Trajectory generation

Usually, it is desirable for the manipulator motion to be smooth with continuous position and velocity for each joint. We can start with trapezoidal velocity function (or line displacement function with two parabolic blends splined together). During the blend portion of the trajectory, velocity profile can be changed according to sine or polynomial functions. We will assume that the blends have the same duration, and therefore the same values of maximum acceleration (modulo a sign).

The blend time and blend range are determined by the peak values of velocity and acceleration according to:

$$t_b = \dot{q}_{\max} / \ddot{q}_{\max}, \quad q_b = 0,5 \ddot{q}_{\max} t_b^2 \quad (1)$$

The linear portion is described by

$$q_{lin} = q_f - q_s - 2q_b \quad (2)$$

If $q_b \geq 0,5(q_f - q_s)$, then $q_b = 0,5(q_f - q_s)$, $t_b = \sqrt{2q_b / \ddot{q}_{\max}}$. (3)

In the case of linear path with parabolic blends (trapezoidal velocity distribution) we can use the following formulas:

for $t < t_s$: $q = q_s$; $\dot{q} = 0$; $\ddot{q} = 0$; (4)

for $t_s < t < t_s + t_b$:

$$q = 0,5 \ddot{q}_{\max} (t - t_s)^2 + q_s, \quad \dot{q} = \ddot{q}_{\max} (t - t_s), \quad \ddot{q} = \ddot{q}_{\max};$$

for $t_s + t_b < t < t_f - t_b$:

$$q = \dot{q}_{\max} (t - t_s - t_b) + q_s + q_b, \quad \dot{q} = \dot{q}_{\max}, \quad \ddot{q} = 0;$$

for $t_f - t_b < t < t_f$

$$q = q_f - 0,5 \ddot{q}_{\max} (t - t_f)^2, \quad \dot{q} = -\ddot{q}_{\max} (t - t_f), \quad \ddot{q} = -\ddot{q}_{\max};$$

for $t > t_f$: $q = q_f$,

$$\dot{q} = 0, \quad \ddot{q} = 0.$$

In the case of linear path with sine-type of blends we can use:

for $t < t_s$: $q = q_s$, $\dot{q} = 0$, $\ddot{q} = 0$;

for $t_s < t < t_s + t_b$

$$q = 0,5 \ddot{q}_{\max} [t - t_s - (t_b/\pi) \sin \pi(t - t_s)/t_b] + q_s,$$

$$\dot{q} = 0,5 \dot{q}_{\max} [1 - \cos \pi(t - t_s)/t_b],$$

$$\ddot{q} = \ddot{q}_{\max} \sin \pi(t - t_s)/t_b;$$

for $t_s + t_b < t < t_f - t_b$:

$$q = \dot{q}_{\max} (t - t_s - t_b) + q_s + q_b,$$

$$\dot{q} = \dot{q}_{\max}, \quad \ddot{q} = 0;$$

for $t_f - t_b < t < t_f$:

$$q = q_f - q_b + 0,5 \dot{q}_{\max} [t - t_f + t_b + (t_b/\pi) \sin \pi(t - t_f + t_b)/t_b],$$

$$\dot{q} = 0,5 \dot{q}_{\max} [1 + \cos \pi(t - t_f + t_b)/t_b],$$

$$\ddot{q} = -\ddot{q}_{\max} \sin \pi(t - t_f + t_b)/t_b;$$

for $t > t_f$: $q = q_f$, $\dot{q} = 0$, $\ddot{q} = 0$. (5)

In the case of n-order polynomial type of velocity profile we can use the following formulas:

$$q = \sum_{i=1}^n \frac{1}{i+1} a_i (t - t_s)^{i+1} + q_s, \quad (6)$$

$$\dot{q} = \sum_{i=1}^n a_i (t - t_s)^i,$$

$$\ddot{q} = \sum_{i=1}^n i a_i (t - t_s)^{i-1}.$$

3. The equations of motions for the manipulator's links

The equations of motions for the i-th link are derived by using the 2nd order Lagrange's equation:

$$\frac{d}{dt} \left(\frac{\partial E_k}{\partial \dot{\theta}_i} \right) - \frac{\partial E_k}{\partial \theta_i} + \frac{\partial E_p}{\partial \theta_i} = M_i(t), \quad i = 1 + 3 \quad (7)$$

If the torsional elasticities in the 4th and 5th joints are considered, the equation (7) derived for i=4 and i=5 can be written in the form:

$$\frac{d}{dt} \left(\frac{\partial E_k}{\partial \dot{\psi}_i} \right) - \frac{\partial E_k}{\partial \psi_i} + \frac{\partial E_p}{\partial \psi_i} = M_i(t), \quad i = 4, 5 \quad (8)$$

where: E_p , E_k - the potential and kinetic energy of the i-th link,

θ_i - the joint angle between the i-1 and i-th link,

$\psi_i = M_i/K_i$ - the torsional deformation defined for the i-th joint,

M_i - the joint drive torque,

K_i - the stiffness coefficient of the joint drive system.

The derivation of these equations for the IRb-60 manipulator's link motions together with the detailed descriptions of the used coefficients can be found in the references [2]. The dynamics equations are presented as the joint torque in terms of the joint position, velocity, and acceleration:

$$M_1(t) = \bar{\theta}_1 \dot{d}_1 + (\bar{\theta}_5 + \bar{\psi}_5) \dot{d}_2 + \dot{\theta}_1 [\dot{\theta}_2 \dot{d}_{10} + \dot{\theta}_3 \dot{d}_{11} + (\dot{\theta}_4 + \dot{\psi}_4) \dot{d}_{12}] + (\dot{\theta}_7 + \dot{\psi}_4) (\dot{\theta}_5 + \dot{\psi}_5) \dot{d}_{13},$$

$$M_2(t) = \bar{\theta}_2 \dot{d}_3 + \bar{\theta}_3 \dot{d}_4 + (\bar{\theta}_4 + \bar{\psi}_4) \dot{d}_5 - 0,5 \dot{\theta}_1^2 \dot{d}_{10} + \dot{\theta}_2^2 \dot{d}_{14} + \dot{\theta}_3 (\dot{\theta}_2 + \dot{\theta}_6) \dot{d}_{15} + (\dot{\theta}_4 + \dot{\psi}_4) [(\dot{\theta}_4 + \dot{\psi}_4) + 2\dot{\theta}_6] \dot{d}_{16} - \dot{\theta}_1 (\dot{\theta}_5 + \dot{\psi}_5) \dot{d}_{13} + \dot{C}_2,$$

$$\begin{aligned}
 M_3(t) &= \bar{\theta}_2 d_4 + \bar{\theta}_3 d_6 + (\bar{\theta}_4 + \bar{\psi}_4) d_7 - 0.5 \dot{\theta}_1^2 d_{11} + \dot{\theta}_2^2 d_{17} + 0.5 \dot{\theta}_3 (\dot{\theta}_2 + \dot{\theta}_6) d_{18} + 0.5 (\dot{\theta}_4 + \dot{\psi}_4) [(\dot{\theta}_4 + \dot{\psi}_4) + 2\dot{\theta}_6] d_{19} - \dot{\theta}_1 (\dot{\theta}_5 + \dot{\psi}_5) d_{13} + G_3, \\
 M_4(t) &= \bar{\theta}_2 d_5 + \bar{\theta}_3 d_7 + (\bar{\theta}_4 + \bar{\psi}_4) d_8 - 0.5 \dot{\theta}_1^2 d_{12} - \dot{\theta}_2^2 d_{16} - 0.5 \dot{\theta}_3 (\dot{\theta}_2 + \dot{\theta}_6) d_{19} - \dot{\theta}_1 (\dot{\theta}_5 + \dot{\psi}_5) d_{13} + K_4 \psi_4 + G_4 \\
 M_5(t) &= \bar{\theta}_1 d_2 + (\bar{\theta}_5 + \bar{\psi}_5) d_9 + \dot{\theta}_1 (\dot{\theta}_7 + \dot{\psi}_4) d_{13} + K_5 \psi_5 \tag{9}
 \end{aligned}$$

where: $\dot{\theta}_6 = \dot{\theta}_2 + \dot{\theta}_3$, $\dot{\theta}_7 = \dot{\theta}_4 + \dot{\theta}_6$, $\bar{\theta}_6 = \bar{\theta}_2 + \bar{\theta}_3$, $\bar{\theta}_7 = \bar{\theta}_4 + \bar{\theta}_6$,
 d_i - the term of centripetal and Coriolis forces, given in [2],
 G_i - the gravity term at the i -th joint.

4. Integration of the equations

The last three equations of the system (9) can be written as

$$M_4(t) = M_{4S} + M_{4D} + M_{4R} \tag{10}$$

$$M_5(t) = M_{5S} + M_{5D} + M_{5R}$$

where: M_{1S} - the static torque caused by gravity loading,

M_{1D} - the dynamic torque caused by inertia forces,

M_{1R} - the additional torque caused by elastic oscillations.

By using the eqs (9) and (10) the following relations can be obtained:

$$M_{4S} = G_4. \tag{11}$$

$$M_{4D} = \bar{\theta}_2 d_5 + \bar{\theta}_3 d_7 + \bar{\theta}_4 d_8 - 0.5 \dot{\theta}_1^2 d_{12} - \dot{\theta}_2^2 d_{16} - 0.5 \dot{\theta}_3 (\dot{\theta}_2 + \dot{\theta}_6) d_{19} - \dot{\theta}_1 \dot{\theta}_5 d_{13},$$

$$M_{4R} = \bar{\psi}_4 d_8 - \dot{\psi}_5 \dot{\theta}_1 d_{13} + K_4 \psi_4,$$

$$M_{5D} = \bar{\theta}_1 d_2 + \bar{\theta}_5 d_9 + \dot{\theta}_1 \dot{\theta}_7 d_{13},$$

$$M_{5R} = \bar{\psi}_5 d_9 + \dot{\psi}_4 \dot{\theta}_1 d_{13} + K_5 \psi_5.$$

Since the mass center of the grasped object is located at the axis z_5 of the end-effector, it can be assumed that $M_{56} = 0$.

The expressions for the joint torques given by equation (11) consist of configuration dependent coefficients multiplied by the instantaneous velocity and acceleration values. When certain simplifying geometries are included it is possible also to factorize an expressions into configuration dependent and independent terms. The goal of these simplifications is to reduce the real time computation of the equations [2].

To obtain the solutions for the manipulator's dynamic equations with time dependent coefficients it is necessary to use numerical integration technique. It was assumed that the torque values in the neighboring time steps are equal

$$M_i(t)^n = M_i(t)^{n-1} \tag{12}$$

The angular acceleration of the oscillation motion in the n -th step can be determined by using the following equations

$$\bar{\psi}_4 = (\dot{\psi}_5 \dot{\theta}_1 d_{13} - K_4 \psi_4 - G_4 - M_{4D} + M_4(t)^{n-1}) / d_8 \tag{13}$$

$$\bar{\psi}_5 = (-\dot{\psi}_4 \dot{\theta}_1 d_{13} - K_5 \psi_5 - M_{5D} + M_5(t)^{n-1}) / d_9$$

The obtained differential equations are 2-nd order, nonhomogenous with the

coefficients dependent on joint coordinates and their derivatives. The numerical integration are performed by using the Runge-Kutta's 4th order method modified by Gil [2]. To use this method it is necessary to transform the system of equations by using the state coordinates

$$Y_1 = \dot{\psi}_4, \quad Y_2 = \dot{\psi}_5, \quad Y_3 = \psi_4, \quad Y_4 = \psi_5 \quad (14)$$

As a result the system of differential equations of the 1st order is obtained

$$dY_1/dt = (\dot{\theta}_1 Y_2 d_{13} - K_4 Y_3 - G_4 - M_{4D} + M_4(t)^{n-1})/d_8 \quad (15)$$

$$dY_2/dt = (-\dot{\theta}_1 Y_1 d_{13} - K_5 Y_4 - M_{5D} + M_5(t)^{n-1})/d_9$$

$$dY_3/dt = Y_1 \quad dY_4/dt = Y_2$$

The boundary conditions for the above equations can be presented in the form:

$$Y_1(0) = 0, \quad Y_2(0) = 0, \quad Y_3(0) = G_4/K_4, \quad Y_4(0) = 0,$$

where $Y_3(0)$ describes the angle of the elastic torsional deformation (in static condition) of the 4th joint drive system at the initial point of motion time.

Under assumption (12) the torque value $M_4(t)^{n-1}$ is generated for the coordinates and their derivatives calculated in the previous step time. This procedure is provided with an error, and obtained satisfactory correct results required to reduce the length of the step time.

5. Experimental measurements for the manipulator's compliances

The torsional stiffness characteristics of the joint drive system are measured by using the test stand with the force and displacement sensors. The recorded results of measurements are linearized by using the least square method, so the values of the stiffness coefficients can be presented (see Table 2).

The acceleration measurements are performed by using the piezo-electric accelerometer DELTA SHEAR-type (Bruel and Kjaer) and recorded by using ENDIM 622.01 (VEB Messapparatenwerk-Schlotheim). The steel cylinder with mass m_0 , radius r_0 , and length h_0 is grasped by the end-effector so that the cylinder symmetry axis is the same as the x_5 axis of the end-effector coordinate system. The accelerometer is mounted inside the cylinder hole (Fig.2).

The measurements are recorded only for the torsional oscillations in the 4th joint drive system with fixed wrist joint ($\theta_5=0$), and fixed arm rotational motion ($\theta_1=0$). The acceleration profiles recorded for the 4th joint drive system are presented in Fig.3 (dotted line). The recorded acceleration profile is considered as the sum of tangent acceleration caused by torsional oscillation, and the x_5 acceleration component of the end-effector global motion, compared with the computer simulation results.

On the basis of the acceleration profiles, obtained experimentally, the amplitude of oscillations can be determined (see Fig.4 and 5). The motion along the given trajectory are performed and recorded many times. The angular velocities are changed step by step with the increment 0,3 1/s. The extreme values in the middle of the oscillation cycle are recorded when the joint torsional velocity is constant.

6. The effects of the compliances in joint drive systems on the accuracy of the performed trajectory

The effects of the compliances existed in the joint drive systems on the accuracy of the performed trajectory can be presented as the quantitative and qualitative differences obtained with stiff and elastic constraints.

Numerical example 1. The trajectory of the wrist center O_3 for the IRb-60 manipulator (see Fig.1) is given be the following data:

$$\begin{array}{lll} x_{03p} = 1,00 \text{ m}, & x_{03k} = 1,60 \text{ m}, & t_{p3} = 0, \\ z_{03p} = 0,65 \text{ m}, & z_{03k} = 1,65 \text{ m}, & v_{03max} = 0,6 \text{ m/s}. \end{array}$$

$$\begin{aligned} \theta_{p1} &= -35^\circ, & \theta_{k1} &= 45^\circ, & t_{p1} &= 0,1 \text{ s}, \\ \theta_{p4} &= -20^\circ, & \theta_{k4} &= -115^\circ, & t_{p4} &= 0, \\ \theta_{p5} &= -90^\circ, & \theta_{k5} &= 40^\circ, & t_{p5} &= 0,05 \text{ s}. \end{aligned}$$

where: t_{pi} - the beginning of the motion time at i -th joint, v_{03max} - the constant velocity of the wrist-center point expressed in the base coordinate system.

The extreme values of the joint torsional oscillations are calculated and shown in the Table 3. The amplitudes of the torsional oscillation of the 4th and 5th joint drive systems are obtained as the functions of the given joint angular velocities. The amplitudes are calculated for 20 different values of velocities with the gradual increments: 0,0785 1/s (for the 4th joint), and 0,131 1/s (for the 5th joint). The computational procedure is repeated 3 times for the following values of the stiffness coefficients: given in the Table 2, decreased by 25%, increased by 25%. The computation results are presented in Fig. 4 and 5.

The velocity functions of amplitudes computed for the 4th and 5th joint drive systems have been quite different. The oscillation motion obtained for the 5th joint is regular, because the mass center of the end-effector with grasped cylinder is located on z_5 axis, and this oscillation motion is independent on the end-effector orientation. The parameter values of the oscillation motion in the 4th joint are dependent on the joint position, velocity, acceleration, and configuration of the manipulator's links. The mean value of amplitude is proportional to the joint velocity.

The natural frequency can be determined from equation (13) transformed into the form:

$$\ddot{\psi}_4 d_8 - \dot{\psi}_5 \dot{\theta}_1 d_{13} + K_4 \psi_4 = 0 \quad (16)$$

$$\ddot{\psi}_5 d_9 + \dot{\psi}_4 \dot{\theta}_1 d_{13} + K_5 \psi_5 = 0$$

and $\nu_4 = (K_4/d_8)^{0,5}$, $\nu_5 = (K_5/d_9)^{0,5}$

The numerical results are: $\nu_4 = 8,398 \text{ rad/s}$, $\nu_5 = 29,393 \text{ rad/s}$.

Table 1. The values of geometrical and mass parameters of the IRb-60 robot manipulator

1	1	2	2p	3	3p	4	5	dim
α_1	$-\pi/2$	0	0	0	0	$-\pi/2$	0	rad
l_1	0,130	0,800	0,800	1,280	0,370	0	0	m
λ_1	0,800	0	0	0	0	0	0,40	m
m_1	282	220	13	30	143	18	63	kg
x_{S1}	-0,125	-0,560	-0,400	-0,708	-0,017	0	0	m
y_{S1}	0,301	-0,050	0	0	0	0	0	m
z_{S1}	0	0	0	0	0	0,041	-0,009	m
I_{x1}	45	28	0,015	0,634	1,110	0,266	0,071	kgm ²
I_{y1}	37	92	9,017	22,03	11,37	0,217	0,671	kgm ²
I_{z1}	44	105	9,024	21,62	11,24	0,152	0,646	kgm ²
$\theta_{1,min}$	-165	-110	-110	45	45	-165	-180	deg
$\theta_{1,max}$	165	-40	-40	155	155	30	180	deg
$\dot{\theta}_{1,max}$	1,57	1,25	1,25	1,13	1,13	1,57	2,62	1/s
$\ddot{\theta}_{1,max}$	2,00	3,00	3,00	3,50	3,50	4,50	4,50	1/s ²

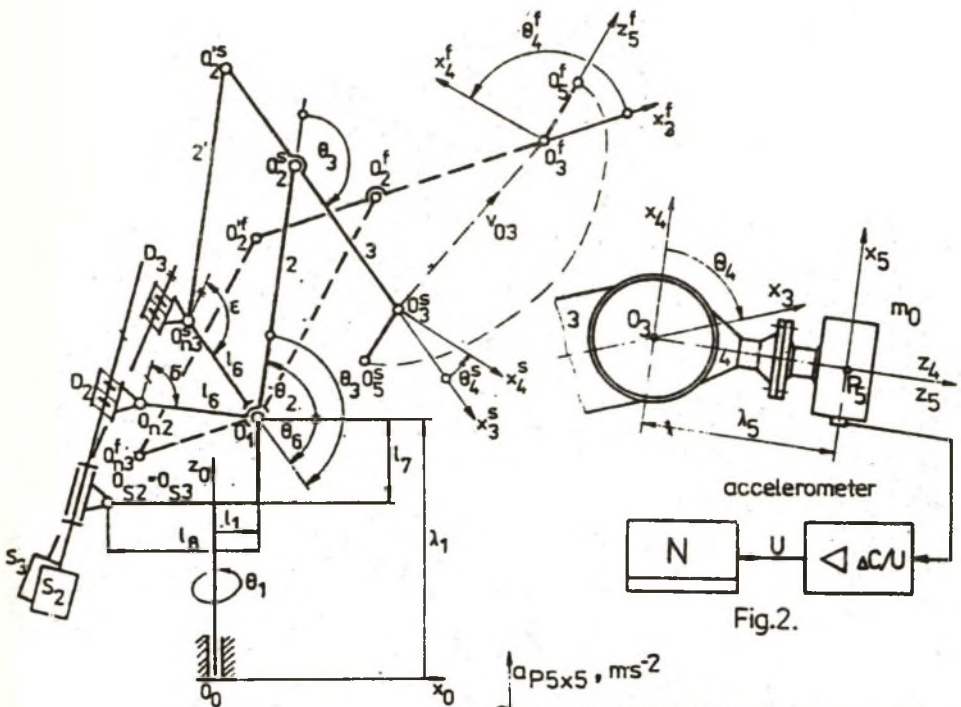


Fig. 1.

Fig. 2.

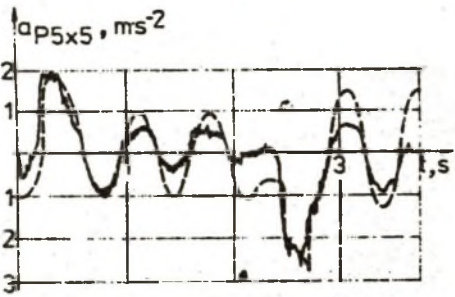


Fig. 3.

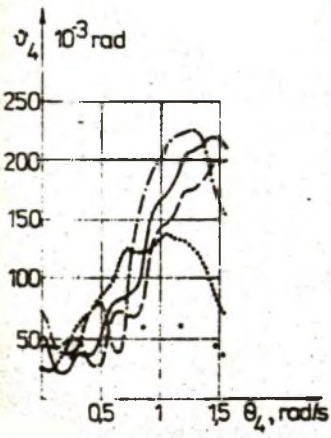


Fig. 4.

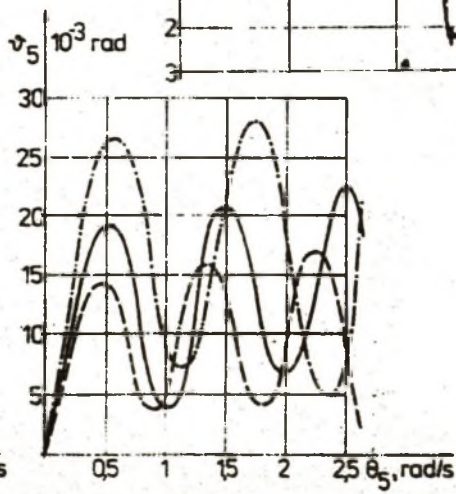


Fig. 5.

Table 2. The stiffness coefficients for the IRb-60 robot. Notations: K -the stiffness coefficient, R -the correlation coefficient.

	1	2	3	4	5
K_i [Nm/rad]	211000	346800	416100	2500	22800
R_i	0.9979	0.9987	0.9978	0.9960	0.9964

Table 3. The simulation results of the torsional motion parameters

i	4			5			
	trapez	sine	polynom	trapez	sine	polynom	dia
$\psi_{i,min}$	-0,1548	-0,1439	-0.1263	-0,0104	-0,0064	-0.0052	rad
$\psi_{i,max}$	0,2622	0,2409	0.1722	0,0091	0,0065	0.0040	rad
$\dot{\psi}_{i,min}$	-0,8629	-1,0347	-0.4015	-0,2511	-0,0958	-0.0639	1/s
$\dot{\psi}_{i,max}$	1,0834	0,9178	0.7082	0,2519	0,0979	0.0720	1/s
$\ddot{\psi}_{i,min}$	-9,4392	-8,9298	-4.6978	-7,6962	-2,2352	-1.8257	1/s ²
$\ddot{\psi}_{i,max}$	8,4777	6,8188	4.5847	7,7060	2,2056	1.3370	1/s ²
ϕ_i	0,4170	0,3848		0,0195	0,0129		rad

7. Conclusion

The dynamic model of the 5R manipulator gave us possibilities to study some effects of the compliances existed in the 4th and 5th joint drive systems on the performed accuracy for the given end-effector trajectory, and on amplitudes of the torsional oscillations. This model used for the IRb-60 manipulator can be useful for another manipulators with the same kinematic scheme.

The amplitudes of oscillations during acceleration and deceleration motions obtained from computer simulation are sufficiently similar to the experimental results. Since the damping was neglected, the calculated results are greater than in reality.

The mathematical model used for computer simulation of the manipulator's dynamics is sufficiently accurate to examine the extreme values of the torsional deflections. The values of amplitudes are proportional to the joint compliances and velocities. These values go up near the resonant frequency. The biggest values of the joint dynamic torques are followed with the deceleration motion.

Excitation of incremental motions in compliant manipulator drive system is determined by nonlinear combinations of gross coordinates and their derivatives. Magnitudes and signs of the kinematically induced components, as well as the overall intensity of the vibratory processes can be modified by changes in the sequencing of segments in trajectory programming as well as by its location in workspace.

The use of polynomial or sine-blends tends to reduce the peak deflection magnitudes while providing the smoother acceleration time functions.

REFERENCES

- [1] ElMaraghy H.A., Johns B.: An Investigation Into the Compliance of SCARA Robots. Part 1: Analytical Model. Part 2: Experimental and Numerical Validation. Trans. ASME, Jnl of Dynamic Systems, Measurement, and Control, March 1986, v.110, pp.18-30.
- [2] Stepniewski A.: Kinematics and Dynamics of the 5R Manipulator with Joint Drive System Torsional Elasticities Taking Into Account. Doct.Diss., Cracow University of Technology, 1989.

- [3] Naganthan G., Soni A.H.: Nonlinear Modeling of Kinematic and Flexibility Effects in Manipulator Design. Trans. ASME, Jnl of Mechanisms, Trans. and Autom. in Design, v.110, Sept.1988, pp. 243-254.
[4] Rivin E.J.: Mechanical Design of Robots. McGraw-Hill, N.York 1987.

WPLYW PODATNOŚCI SKRĘTNEJ UKŁADÓW NAPEĐOWYCH PRZEGUBÓW MANIPULATORA
NA DOKŁADNOŚĆ REALIZOWANEJ TRAJEKTORII

Streszczenie

Dla manipulatora IRb-60 przedstawiono równania ruchu członów przy uwzględnieniu podatności skrętnej układów napędowych 4- i 5-go przegubu. Zarejestrowany przebieg przyspieszenia punktu chwytaka porównano z wynikami symulacji komputerowej oraz analizowano wpływ podatności i charakterystyk zadawanego ruchu w przegubach na dokładność robota.

EINFLUSS DER DREHELASTIZITÄT VON ANTRIEBERSELEMENTEN DER GELENKEN
DES MANIPULATORS AUF DIE GENAUIGKEIT DER REALISIERTEN TRAJEKTORIE

Zusammenfassung

Für den Manipulator IRb-60 wurden die Bewegungsgleichungen der Glieder unter Berücksichtigung der Drehelastizität des vierten und fünften Gliedes vorgelegt. Verglichen wurden: der registrierte und der durch rechnergestützte Simulation gefundene Verlauf von Beschleunigung eines Greiferpunktes. Untersucht wurde Einfluss der Elastizität und der Eigenschaften von vorgegebener Bewegung in den Gelenken auf die Genauigkeit des Roboters.

Wpłynęło do redakcji w styczniu 1992 r.

Recenzent: Jan Kaźmierczak